DAMAGE TOLERANCE OF A GEODESICALLY STIFFENED ADVANCED COMPOSITE STRUCTURAL CONCEPT FOR AIRCRAFT STRUCTURAL APPLICATIONS

Marshall Rouse and Damodar R. Ambur
NASA Langley Research Center
Hampton, VA 23665-5225

INTRODUCTION

Geodesically stiffened structures that utilize continuous filament composite materials for stiffener construction are very efficient for aircraft fuselage applications since this structural concept is very effective in carrying loads due to bending, shear, torsion, and internal pressure. Structural efficiency combined with cost effective methods of manufacturing make geodesically stiffened structures very attractive for commercial transport structural applications. Geodesically stiffened structures are also very damage tolerant since there are multiple load paths available due to the nonprismatic nature of the structure that can help redistribute the load. The potential of geodesically stiffened composite structures for a fuselage application that utilizes advanced manufacturing processes needs to be demonstrated to add to the information base on these structural concepts for aircraft.

This paper describes the features of a geodesically stiffened panel concept that was designed for a fuselage application with a combined axial compression loading of 3,000 lb/in. and a shear loading of 600 lb/in. Specimens representative of this panel concept have been tested in uniaxial compression both without and with low-speed impact damage to study the buckling and postbuckling response of the structure. Experimental results that describe the stiffness and failure characteristics of undamaged and impacted damage specimens are presented. A finite element analysis model that captures the principal details of the specimens has been developed and used to predict the panel response. Analytical results on panel end-shortening are compared with the experimental results. Analytical results that describe panel end-shortening, out-of-plane displacement and stress resultants are presented.

SPECIMEN DESCRIPTION

The specimens tested in this investigation were fabricated from commercially available Hercules Incorporated AS4 graphite fiber preimpregnated with Hercules 3502 epoxy resin (AS4/3502). The skins of the specimens were made from 12 K tow material with a [±45/90/∓45] stacking sequence. The skins of the specimens had a fiber cross-over pattern across the mid-section of the panel to simulate a filament wound skin feature. The stiffeners were placed at ±20° to the longitudinal axis of the test panel. The stiffeners were made of unidirectional tows of graphite-epoxy material overwrapped with graphite-epoxy fabric material and were secondarily bonded to the skin. Two frame clips were made of woven graphite-epoxy fabric and secondarily bonded to the skin at a distance of 10 inches on either side of the horizontal centerline of the specimen. Also, a buffer strip made from unidirectional tow material was embedded in the skin at the location of the frame clips to simulate a fail-safe strap in a fuselage. A total of three specimens was tested in this investigation. All of the specimens had a 40-inch length. Two of the specimens were 14.56 inches wide and the third was 29.12 inches wide. The ends of the specimens were potted and ground flat and parallel for uniform load introduction. The sides of the specimens were supported with knife-edges. A sketch of the test specimen including the local details is shown in figure 1.

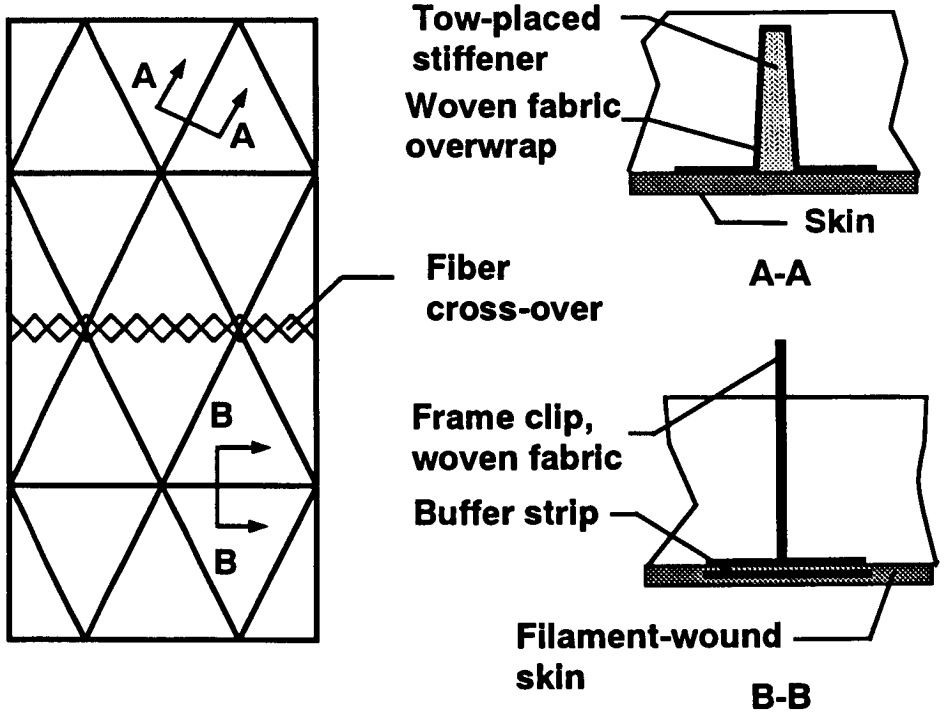

Figure 1. Specimen description

A summary of results for all of the panels that was tested without impact damage is shown in Figure 2. The panels were loaded in compression using a one million pounds capacity hydraulic test machine. Applied load P normalized by the width of the test section b plotted as a function of end-shortening u normalized by the length of the test section L is shown on the left of the figure. Results for the 29.12- and 14.56-inch-wide panels are represented by the circles and the squares, respectively. The theoretical buckling load is indicated by the open symbols. The experimental failure load of the panel is indicated by the filled symbols. The panels buckled at a normalized applied load of approximately 1400 lb/in. All of the panels tested without damage failed at a value of applied load greater than the analytical buckling load. The 29.12-inch-wide panel failed at a value of normalized applied load of 3,312 lb/in. The 14.56-inch-wide panel failed at a value of normalized applied load of 3,540 lb/in.

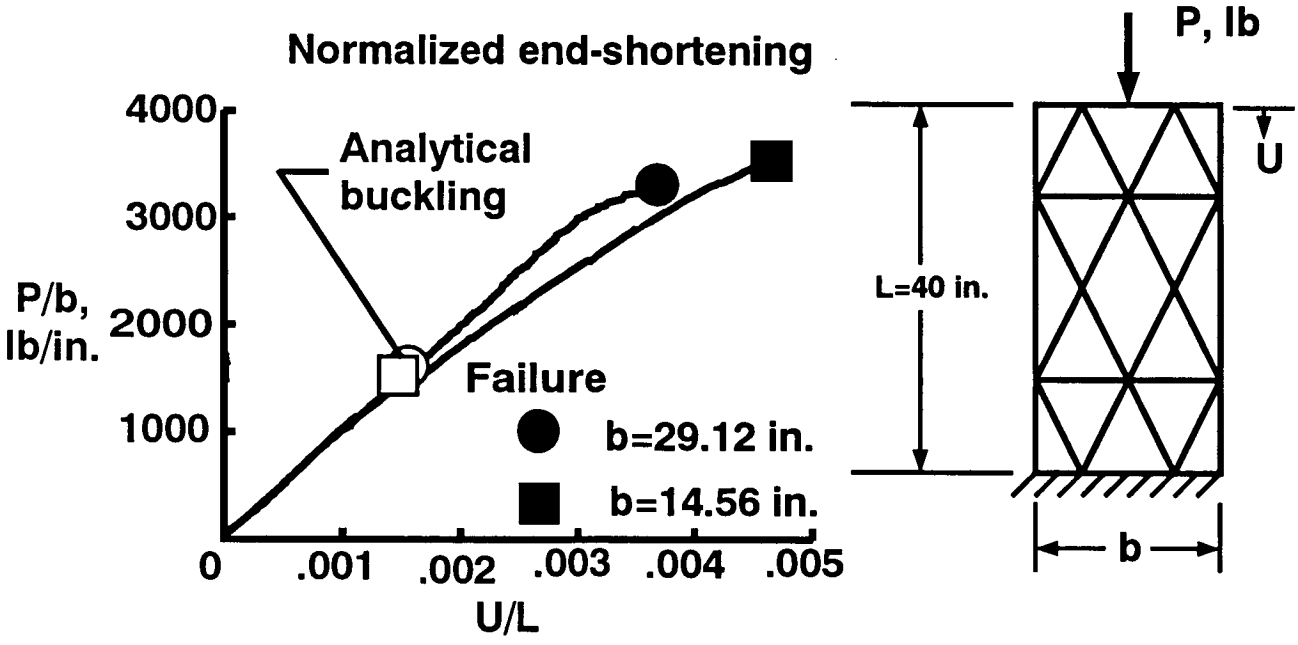

Figure 2. Summary of results for specimens tested without impact damage

Out-of-plane deflection w measured at the intersection of a frame and stiffeners located at the midlength of the panel normalized by the skin thickness t is shown in Figure 3 as a function of normalized load. Failure of the panels is indicated by the filled circles. All of the panels deformed out of plane prior to buckling when loaded. The 29.12-inch-wide specimen exhibited the most out-of-plane deflection during loading with a maximum value of over 6 times the skin thickness. The 14.56-inch-wide panel had a maximum out-of-plane deflection of approximately 4 times the skin thickness.

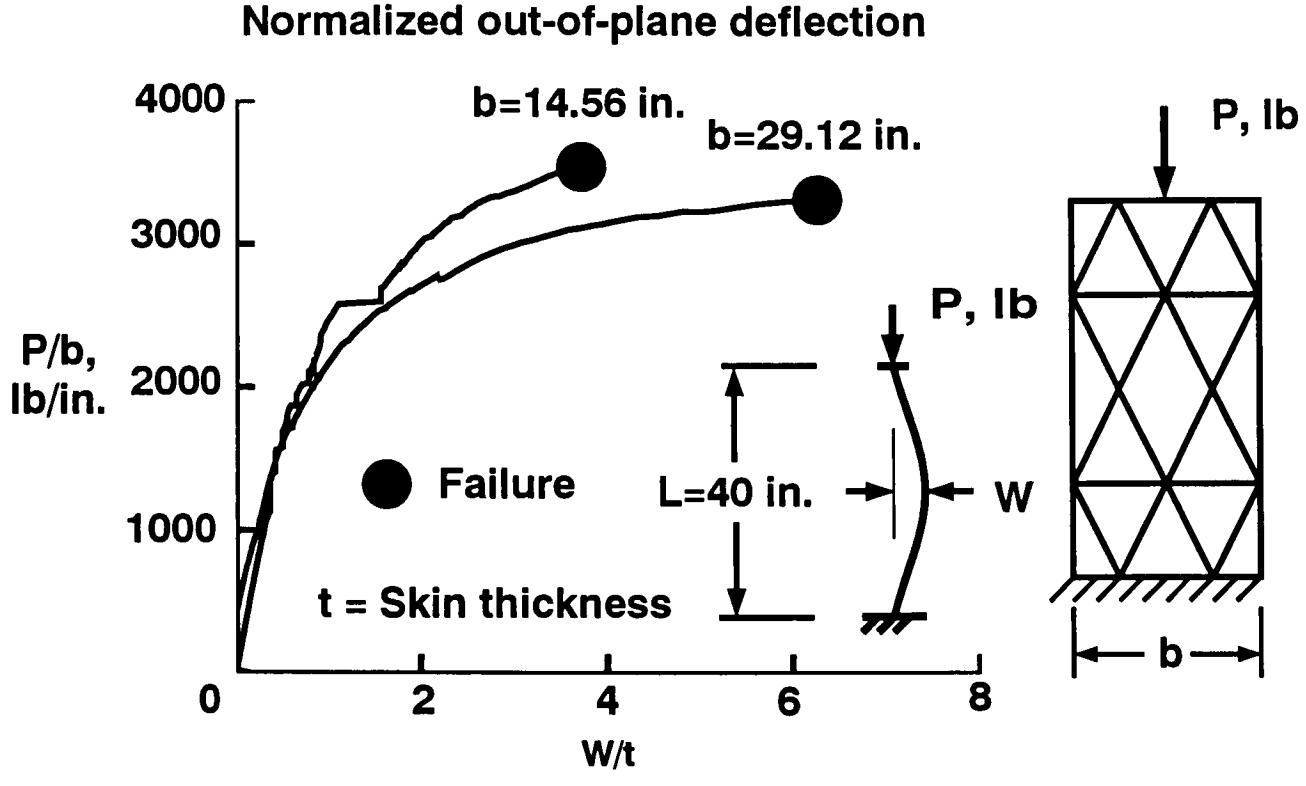

Figure 3. Out-of-plane deflection results for specimens tested without impact damage

SKIN SURFACE STRAIN

A comparison of typical surface strain results for a 14.56-inch-wide panel tested without impact damage is presented in Figure 4 as a function of normalized load. The surface strain ε_x results were recorded from back-to-back strain gages oriented parallel to the direction of applied loading at two locations on the skin. Surface strain results from back-to-back strain gages at location A, which is at the center of the specimen on the skin, are indicated by the filled circles. Surface strain results from back-to-back strain gages at location B, which is away form the center of specimen on the skin, are indicated by the filled square. The panel had a maximum compressive strain of approximately 0.008 in./in. and a maximum tensile strain of approximately 0.002 in./in. at the center of the specimen at failure. The divergence of the back-to-back strain gage results at the center of the panel suggests that bending strain at the center of the specimen is due to local buckling of the skin as the panel was loaded to failure. The discontinuities in the surface strain results measured at the center of the panel suggest that a redistribution of load occurred at approximate values for normalized load of 1,500 lb/in. and 2,500 lb/in. The redistribution of load was due to a combination of changes in skin local buckling mode and local failures at the skin-stiffener interface and fiber cross-over region. This local damage could have resulted in redistribution of load near location B which is indicated by sudden reductions in strain at 1500 lb/in. and 2,500 lb/in. The panel had a maximum compressive strain of approximately 0.001 in./in. at location B. The discontinuities in the load-strain curve for surface strain results measured at location B suggest that local failures caused redistribution of load in the panel as it was loaded to failure.

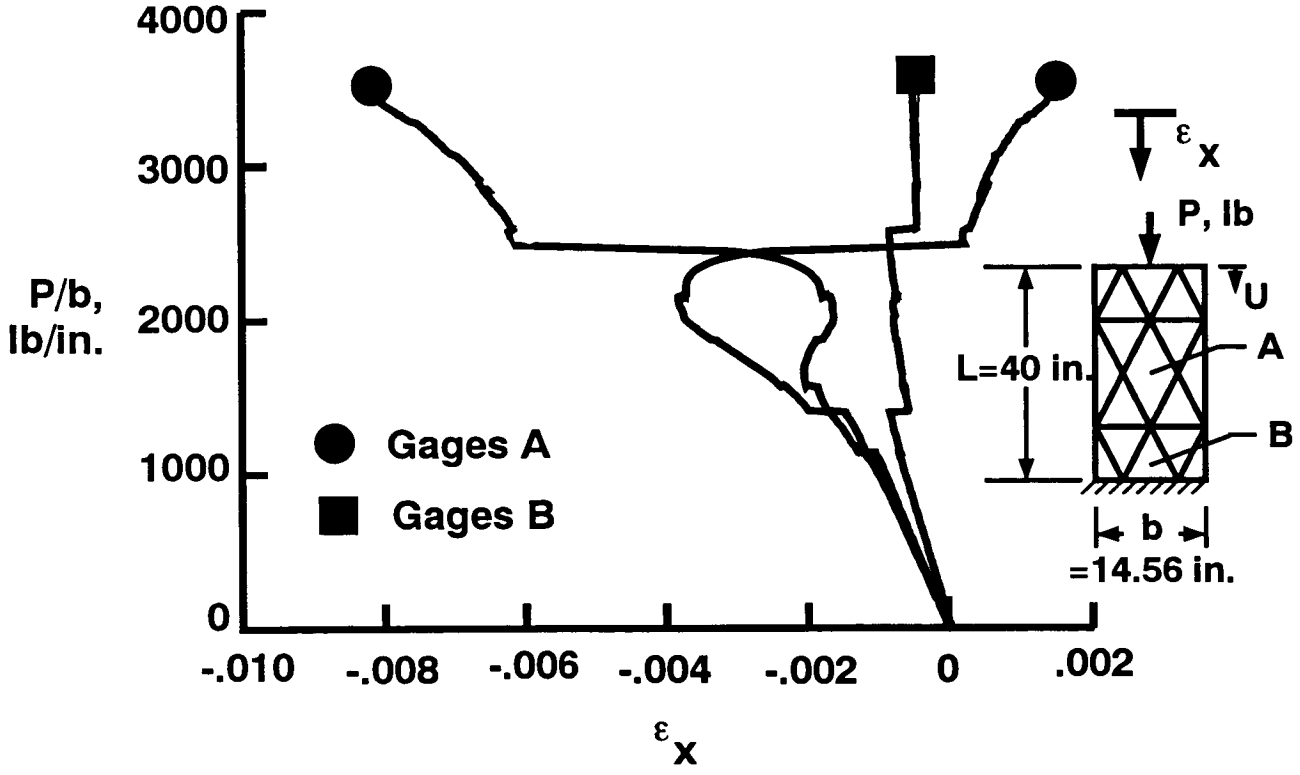

Figure 4. Typrical surface strain results for a 14.56-inch-wide panel

STIFFENER AXIAL STRAIN

Typical stiffener axial strain results for a 14.56-inch-wide panel tested without impact damage are presented in Figure 5 as a function of the normalized applied load. The axial strain ε results were recorded from strain gages oriented parallel to the direction of the stiffener at locations midway between stiffener intersections. Axial strain data at location A on the crown of the stiffener are indicated by the filled circle. Surface strain data on the skin below the stiffener are indicated by the filled square. Axial strain data at locations C on the sides of the stiffener are indicated by the filled diamond. A maximum tensile strain at failure of approximately 0.0005 in./in. was measured at location A. The panel had a maximum compressive strain at Location B of approximately 0.0047 in./in. at failure. Divergence of the axial strain data at locations A and B suggests that bending strains occurred about a plane parallel to the mid plane of the skin as it was loaded into the postbuckling range. The panel had a maximum compressive strain value at locations C of approximately 0.002 in./in. at failure. The results at locations C also suggest that no lateral bending of the stiffener occurred. Also, the discontinuities in the load-strain curves shown in Figure 5 suggest that a redistribution of load occurred in the panel due to local failures prior to the failure of the panel.

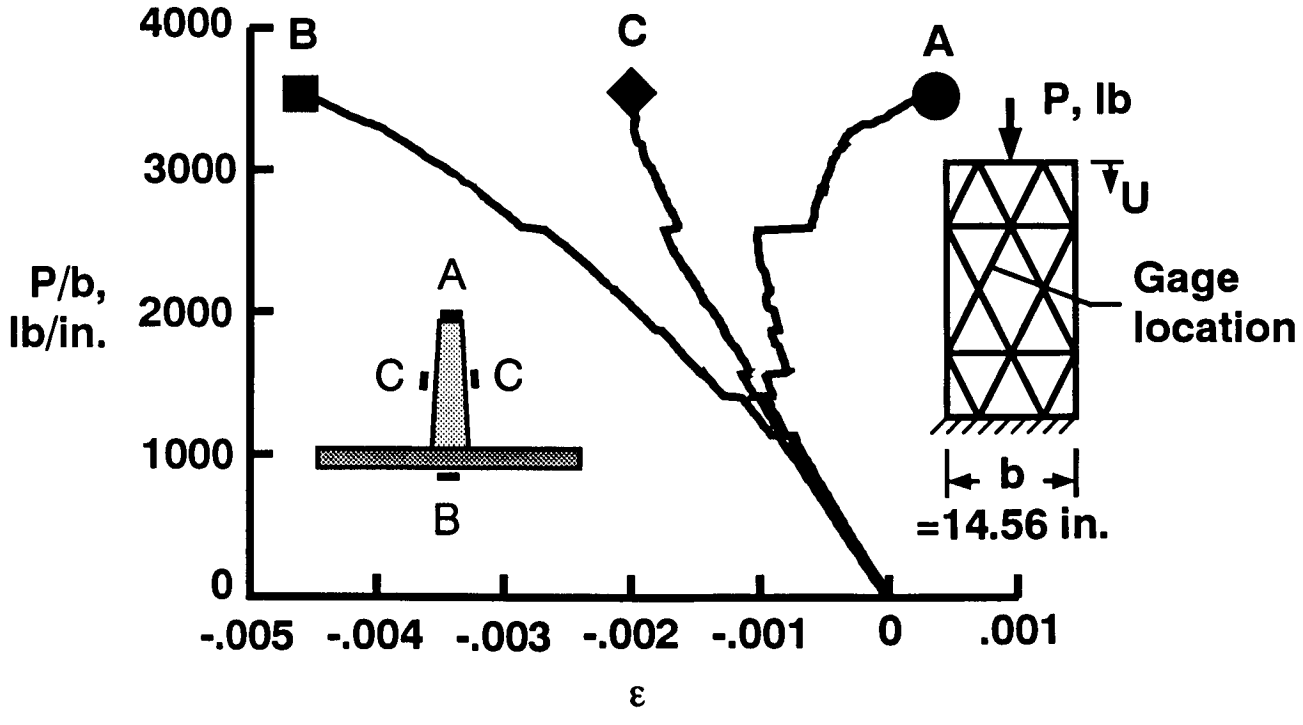

Figure 5. Typical axial strain results for a 14.56-inch-wide panel

FAILURE OF GEODESICALLY STIFFENED COMPRESSION PANELS

Typical failure characteristics of the geodesically stiffened compression panel tested without impact damage are shown in Figure 6. The photograph on the left of the figure shows the skin side of the failed panel. The panel failed due to separation of the skin from the stiffeners across the middle of the panel in addition to the failure along the fiber cross-over region. The photograph on the right of the figure shows a close-up of the local failure mode of the panel. The skin-stiffener separation at a stiffener intersection is shown here.

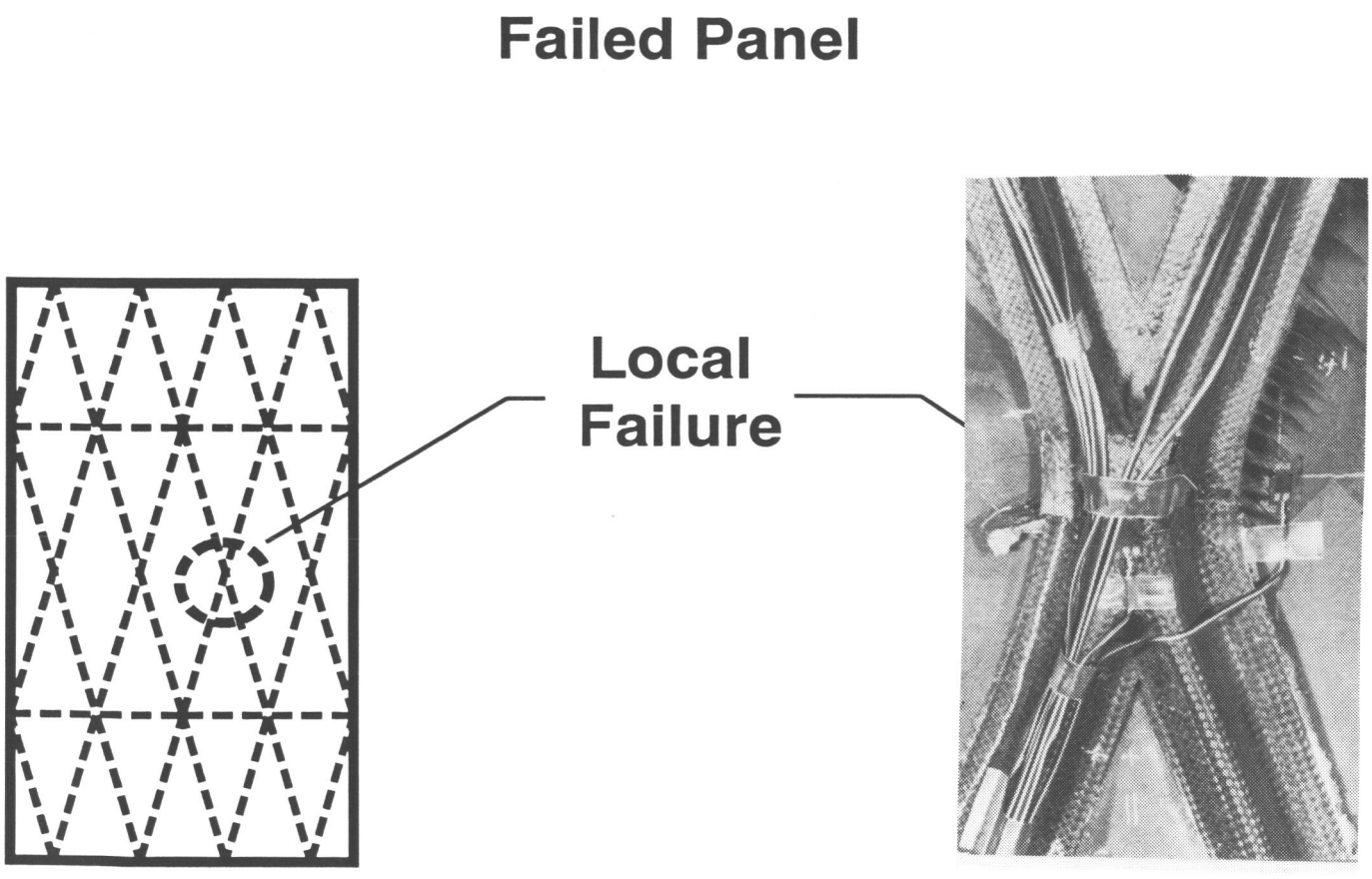

Figure 6. Failure characteristics of a geodesically stiffened compression panel

LOW-SPEED IMPACT DAMAGE OF GEODESICALLY STIFFENED COMPRESSION PANELS

Experimental results for a geodesically stiffened compression panel subjected to low-speed impact damage are presented in Figure 7. A 14.56-inch-wide panel was subjected to low-speed impact damage at two locations near the skin-stiffener interface prior to testing. Aluminum spheres 0.5 inches in diameter were used as the impact projectile in this investigation. The panel was impacted at a point midway between intersecting stiffeners at a velocity V_1 of 345 ft/sec and at the intersection of two stiffeners at a velocity V_2 of 350 ft/sec. The plot on the left of the figure shows normalized end-shortening as a function of normalized applied load. Failure of the undamaged and impact damaged panels are represented by the filled circles. The analytical buckling load of an undamaged panel is represented by the open circle. The results show that the impact damaged panel failed at a value of normalized load of approximately 2,900 lb/in. which is slightly lower than the failure load of the panel tested without low-speed impact damage. The photograph on the right of the figure shows the failed impact damaged panel. The photograph shows that the panel failed in a similar mode to the undamaged panel that was described in Figure 6. The results presented in figure 7 suggest that the presence of low-speed impact damage did not significantly influence the stiffness or strength of this geodesically stiffened compression panel.

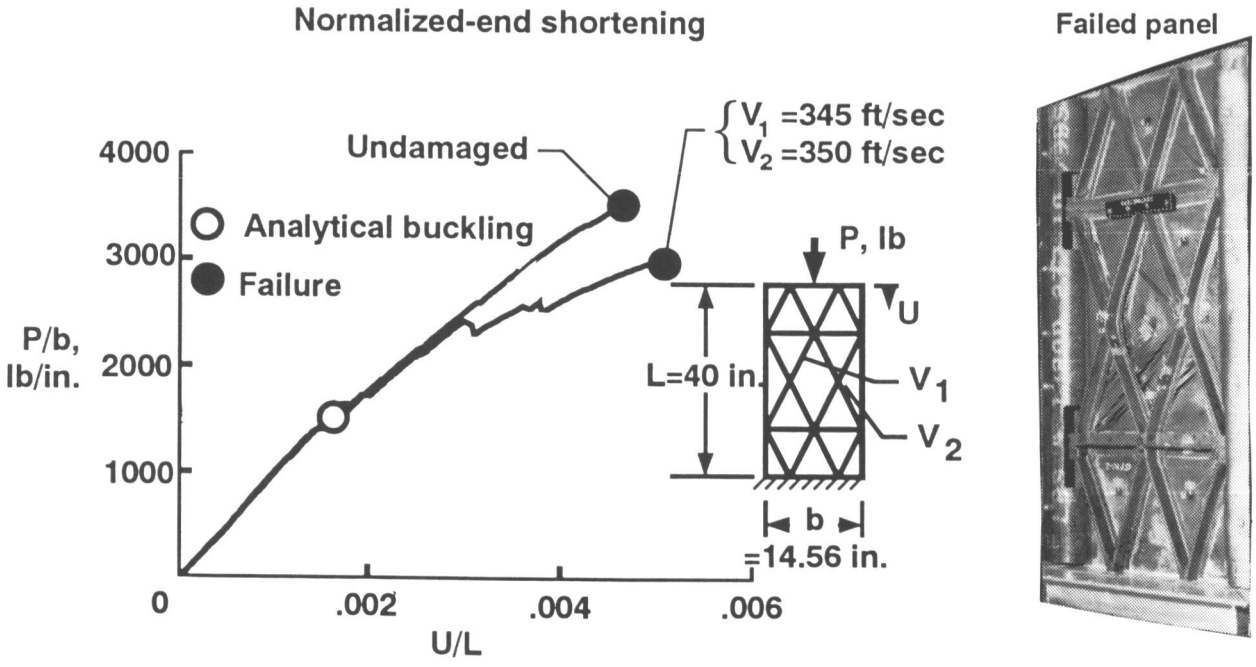

Figure 7. Summary of results for panels tested with low-speed impact damage

GEODESICALLY STIFFENED COMPRESSION PANEL TEST AND ANALYSIS CORRELATION

A comparison between test results and analytical results obtained using the Computational Mechanics Testbed (COMET) finite element computer code (ref. 1) is presented in Figure 8. A finite element analysis was used to perform linear and geometrically nonlinear calculations. The skin, stiffeners, and frame clips were modeled with quadrilateral plate elements that allow transverse shear deformations. The finite element model of the 14.56-inch-wide panel had approximately 18,000 degrees of freedom. Boundary conditions shown in Figure 8 were assumed along the loaded edges of the panel. A uniform edge displacement u was applied to the loaded edge of the panel and this degree of freedom was constrained at the opposite edge. The applied load was calculated by summing the reactions along the constrained edge of the panel. Out-of-plane deflections w were constrained along the edges of the panel. Normalized end-shortening results as a function of normalized load are shown on the left of the figure. The circles represent experimental results and the line represents analytical results. The filled circle denotes failure of the panel and the filled square denotes the analytical buckling load obtained from linear buckling calculations. End-shortening contours calculated from a geometrically nonlinear finite element analysis are shown on the right of the figure. The contour results indicate that end-shortening was uniform across the width at the loaded edges of the panel. However, the end-shortening contours were not uniform across the width of the panel away from the loaded edges. The results suggest that the end-shortening contours were influenced by the stiffeners and stiffener intersection points. The results presented in Figure 8 indicate that the analysis accurately predicts buckling and postbuckling response of the panel up to about two times the buckling load.

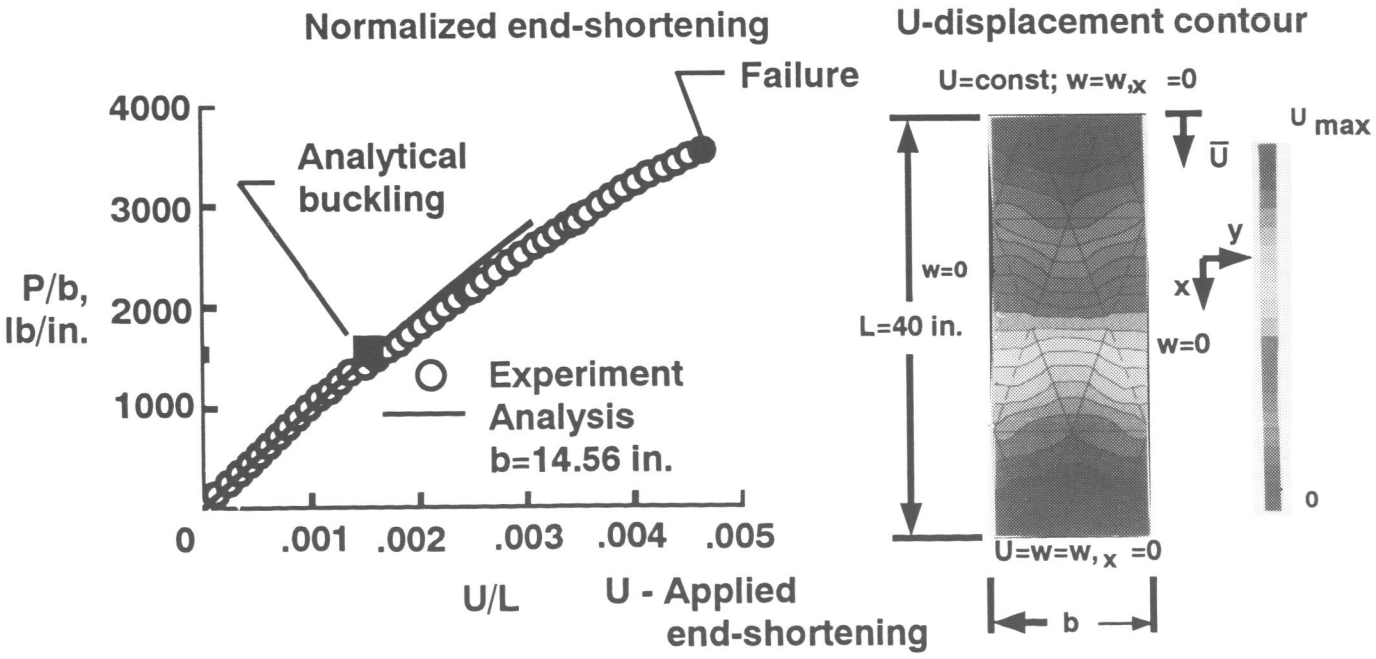

Figure 8. Comparison of experimental and analytical end-shortening results

GEODESICALLY STIFFENED COMPRESSION PANEL OUT-OF-PLANE DEFLECTION CONTOURS

Finite element results of out-of-plane deflections w at approximately 1.5 times the buckling load and a photograph of the corresponding moire-fringe pattern are presented in Figure 9. A photograph of the moire-fringe pattern on the skin side of a 14.56-inch-wide panel is shown on the left of the figure. This photograph shows that the rhombic skin panel buckled into three halfwaves at the center of the panel. The analytical out-of-plane deflection contours viewed from the stiffener side of the panel presented on the right of the figure compare well with experimental results. The out-of-plane deflection results presented in the figure also indicate that the center region of the entire panel deformed out-of-plane during loading. Also, the buckle pattern exhibits a noticeable skew.

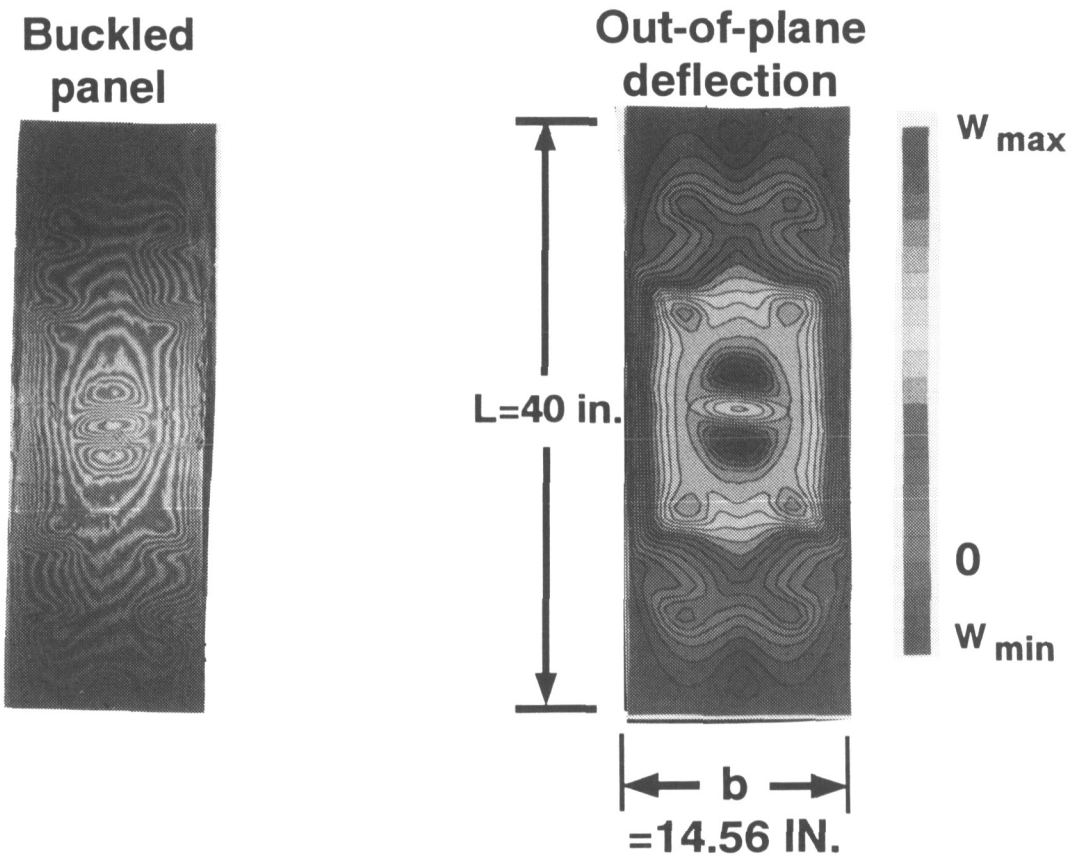

Figure 9. Experimental and analytical out-of-plane deflection results.

TYPICAL STRESS RESULTANT CONTOUR RESULTS

Typical stress resultant contours for a 14.56-inch-wide specimen calculated from a geometrically nonlinear finite element analysis at approximately 1.5 times the buckling load are presented in Figure 10. Contour plots of the inplane normal stress resultants N_x in a direction parallel to the longitudinal axis of the panel and along the axis of the stiffeners and frame clips are shown on the left of the figure. The contour results indicate that most of the compression load is carried by the stiffeners of the geodesic compression panel. Contour plots of the inplane normal stress resultants N_y (in a direction normal to the longitudinal axis of the panel) are shown on the middle of the figure. These results indicate that the stress resultants normal to the longitudinal axis of the panel are a maximum near the location of frame clips where the 0° material buffer strip was embedded into the skin laminate. The high N_y stress resultants at the location of the frame clips is due to the buffer strips resisting the lateral movement of the stiffeners at the stiffener intersections. Contour plots of the inplane shear stress resultants N_{xy} are shown on the right of the figure. Inplane shear stress resultant contour results indicate that shear stresses are generated in the skin although the panel is loaded in uniaxial compression. These inplane shear stresses in the skin caused the skewed buckle pattern described in Figure 9.

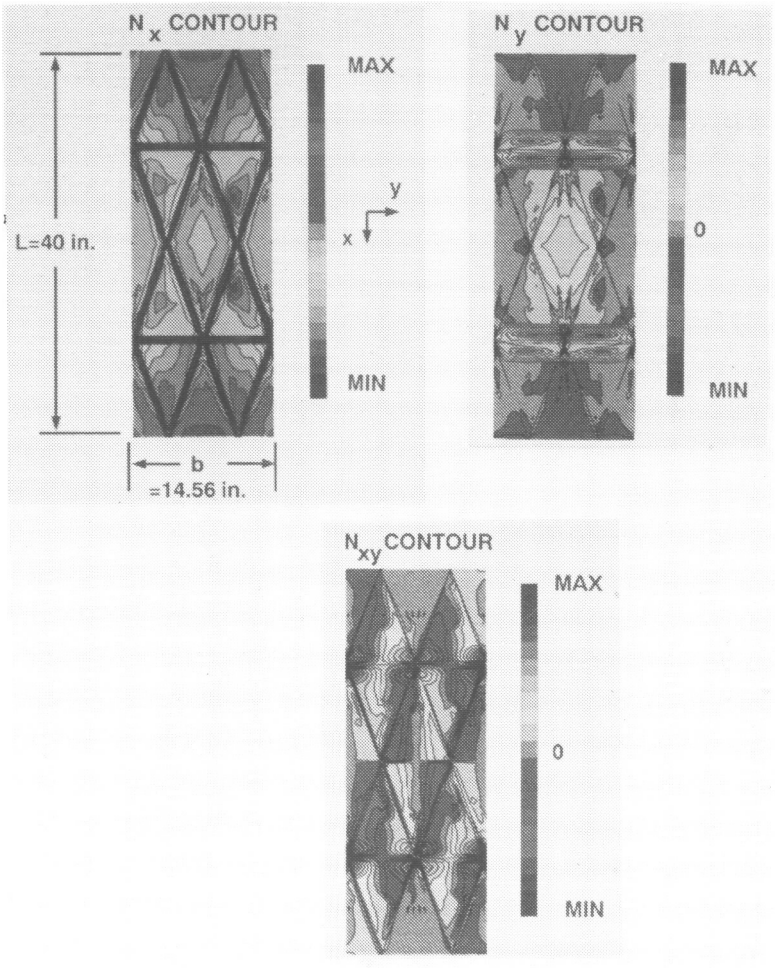

Figure 10. Typical stress resultant contour results.